

1 **Kinetic study of glyphosate degradation in wet air oxidation**

2 **conditions**

3 Dan Feng^a, Laure Malleret^b, Audrey Soric^a, Olivier Boutin^{a,*}

4 ^a Aix Marseille University, CNRS, Centrale Marseille, M2P2, Marseille, France

5 ^b Aix Marseille University, CNRS, LCE, Marseille, France

6

7 **Abstract**

8 Glyphosate is one of the most widely used herbicides in the world against perennial and
9 annual weeds. It has been reported to be a micro pollutant, and its degradation in
10 different wastewater treatment processes must be studied. For that purpose, the kinetics
11 of wet air oxidation of glyphosate was studied in an autoclave reactor at a temperature
12 range of 423-523 K and under a total pressure of 15 MPa. Oxidation reactions obeyed
13 the first-order kinetics with respect to glyphosate concentration. The activation energy
14 for glyphosate oxidation was found to be equal to 68.4 kJ mol⁻¹. Furthermore, the
15 possible reaction intermediates and main end products of glyphosate degradation in the
16 wet air oxidation process were identified and quantified using UV-spectrophotometry
17 and liquid chromatography coupled to high resolution mass spectrometry. A
18 degradation pathway for glyphosate oxidation was proposed.

19

20 *Keywords:* Glyphosate; wet air oxidation; kinetics; emerging contaminant

* Corresponding author. Aix Marseille University, CNRS, Centrale Marseille, M2P2, Marseille, France.
E-mail address: olivier.boutin@univ-amu.fr (O. Boutin)

21 **1 Introduction**

22 Glyphosate (*N*-(phosphonomethyl)glycine), a synthetic phosphonate compound,
23 is a broad-spectrum, post-emergence and non-selective organophosphate herbicide
24 (Manassero et al., 2010; Gill et al., 2017). Glyphosate is one of the most widely used
25 herbicides in the world against perennial and annual weeds and the active ingredient of
26 Roundup (Baylis, 2000; Chen and Liu, 2007). Due to the numerous uses of glyphosate,
27 it has been widely detected in the aquatic environment with potential toxicity to non-
28 target aquatic life (Guilherme et al., 2010; Sandy et al., 2013). Therefore, it has attracted
29 much attention in recent years in order to avoid further risks and effectively avoid it in
30 the environment.

31 Various conventional methods have been applied to treat glyphosate-containing
32 wastewater, such as precipitation, membrane filtration, adsorption and biodegradation
33 (Xie et al., 2010; Liu et al., 2013; Herath et al., 2016; Firdous et al., 2017). However,
34 these processes may cause secondary pollution, such as the generation of sludge (Wang
35 et al., 2016). The safe disposal of sludge is another issue in wastewater treatment.
36 Furthermore, biological treatment generally needs a long residence time to obtain high
37 glyphosate removal efficiency up to 90% (Fan et al., 2012; Hadi et al., 2013). Thus,
38 more efficient technology for glyphosate degradation is needed to be developed. In this
39 work, the conditions to use wet air oxidation (WAO) as an efficient process were studied.
40 This process would be more dedicated to treating effluents from the pesticides industry,
41 or other types of effluents with rather high pollutants concentration, before their release
42 in the environment. The first industrial development of this process was in the 60's.

43 The principal of WAO is to oxidize organic pollutants at high temperature and
44 pressure through the generation of active oxygen species, such as hydroxyl radicals. It
45 has been proven to be a potential treatment technology for wastewaters containing a
46 high content of organic contaminants or toxic pollutants when direct biological
47 treatment is unfeasible (Levec and Pintar, 2007). Typical conditions of WAO are 398-
48 573 K for temperature and 0.5-20 MPa for pressure (Debellefontaine and Foussard,
49 2000; Lefevre et al., 2012; Lefèvre et al., 2011a, 2011b). By using oxygen or air as the
50 oxidizing agent, WAO method can effectively converts organic pollutants to CO₂ and
51 H₂O and usually less toxic oxidation intermediates up to short-chain acids (Hu et al.,
52 2001; Luck, 1999; Mishra et al., 1995). For a further degradation of short-chain acids,
53 such as acetic acid, supercritical water or a catalytic system is needed, or a biological
54 process (Watanabe et al., 2001). Under high temperatures and pressures, the solubility
55 of oxygen is enhanced in aqueous solutions, which provides a strong driving force for
56 oxidation (Demirel and Kayan, 2012). For industrial applications, the design of bubble
57 columns working at high pressure and high temperature has been yet studied (Feng et
58 al., 2019; Leonard et al., 2019, 2015).

59 Table S1 summarizes available studies on the treatment of pollutants by WAO
60 process. It is shown that WAO technology could achieve high removals of organic
61 compounds and of total organic carbon (TOC). The performance of WAO can be
62 affected by three main parameters: temperature, oxygen partial pressure (and also total
63 pressure) and reaction time. With the increase of temperature, the removal efficiency of
64 organic compounds generally increases (García-Molina et al., 2007; Lefèvre et al.,

2011a; Lei et al., 2007; Mantzavinos et al., 1996). For instance, the removal of 4-chlorophenol ranges from 1.1% to 99.5% with temperature increasing from 423 to 463 K (García-Molina et al., 2007). The partial pressure of oxygen is part of the driving force for mass transfer, thus the removal efficiency increases with the increase in oxygen amount (Lei et al., 2007; Mantzavinos et al., 1996). However, if the stoichiometric quantity of oxygen is achieved, the oxygen partial pressure is not a significant factor for organic compounds degradation (Kim and Ihm, 2011; Lei et al., 2007). With increasing reaction time, more free radicals are generated, which promotes the degradation rate (Demirel and Kayan, 2012; Lefèvre et al., 2011a; Shende and Levec, 1999). Although WAO technology has been frequently used for the treatment of organic pollutants, most studies focus on phenolic compounds. Little literature studies the degradation of glyphosate via WAO technology. Only Xing et al. (2018) reports that 100% glyphosate removal and over 93% organic phosphorus removal (containing 200-3000 mg L⁻¹ glyphosate) is achieved for real glyphosate wastewater by catalytic wet oxidation using modified activated carbon as a catalyst. The reactor is a co-current upflow fixed bed reactor at 383-403 K and under 1.0 MPa with a residence time of 4.8 h. There is no literature focuses on the kinetics of glyphosate oxidation by WAO technology, which is necessary for the design of WAO reactor.

Several studies show two possible oxidation pathways of glyphosate under other oxidation conditions, such as photodegradation (Chen et al., 2007; Echavia et al., 2009), manganese oxidation (Barrett and McBride, 2005) and H₂O₂/UV oxidation (Manassero et al., 2010): (1) glyphosate transfers to aminomethylphosphonic acid (AMPA) through

87 the cleavage of C-N bond; (2) glyphosate converts to sarcosine through the direct
88 cleavage of C-P bond. AMPA may be further oxidized to methylamine, formaldehyde,
89 NH_4^+ , NO_3^- and PO_4^{3-} . Sarcosine could be further oxidized to glycine, formaldehyde,
90 and NH_4^+ . Studies on oxidation pathways of glyphosate by WAO process is rare. Only
91 Xing et al. (2018) suggest the AMPA pathways for glyphosate degradation by catalytic
92 wet oxidation.

93 Therefore, this work investigates the wet air oxidation of glyphosate synthetic
94 solutions up to 1 g.L^{-1} in an autoclave batch reactor under three temperatures (423, 473
95 and 523 K) and a pressure of 15 MPa. The kinetics of glyphosate degradation by WAO
96 process is carried out at the three temperatures, to enable the determination of the
97 removal efficiencies, the rate constants and the activation energy of the oxidation
98 reaction. A kinetic model is determined to represent the experimental data for
99 glyphosate. Some possible transformation products of glyphosate are also searched and
100 measured by using UV-spectrophotometry and liquid chromatography coupled to high
101 resolution mass spectrometry, in order to identify the main by-products formed and to
102 propose a possible oxidation pathway of glyphosate by WAO process.

103

104 **2 Materials and methods**

105 2.1 Chemicals

106 Glyphosate is purchased from Leap Labchem Co., Limited, China with a purity
107 higher than 95%. AMPA and glyoxylic acid are obtained from Sigma-Aldrich (Saint
108 Quentin Fallavier, France). Aqueous stock solutions (1 g.L^{-1}) are prepared in

109 polypropylene bottles, as well as standards and injection solutions. All other chemicals
110 and solvents used are also obtained from Sigma-Aldrich. The synthetic air (purity
111 higher than 99.999%) used as oxidant is bought from Air Liquid, France.

112

113 2.2 Experimental procedure

114 In order to study the kinetics of glyphosate degradation, the experiments are
115 conducted in a batch reactor (Top Industrie, France). The experimental apparatus for
116 WAO in the batch reactor is shown schematically in Fig. S1. The autoclave with an
117 internal volume of 202 mL can reach a maximum pressure and temperature of 30 MPa
118 and 623 K, respectively. The temperature in the reactor is regulated by a hot (electric
119 power)/cold (double jacket with air or water) regulating system. The stirring device is
120 a rushton type mixer with 8 blades, with a hollow shaft allowing recirculation of the
121 gas phase into the liquid phase. Experimentally, the reactor is first pressurized with an
122 amount of nitrogen, which value is estimated from thermodynamic calculations using
123 the Soave-Redlich-Kwong equation of state (Lefèvre et al., 2011b), in order to reach
124 desired final pressure and temperature. To evaluate the influence of the temperature on
125 glyphosate oxidation by WAO process, reactions with an initial glyphosate
126 concentration of 1 g L⁻¹ are conducted at three temperatures (423, 473 and 523 K). This
127 concentration of glyphosate is in the range of glyphosate concentration measured in
128 industrial wastewaters (Heitkamp et al., 1992; Xing et al., 2017). The initial pressure
129 of nitrogen is 7.78, 6 and 2.15 MPa with respect to the temperature of 423, 473 and 523
130 K, respectively. 120 mL glyphosate solution is injected into the reactor and then the

131 reactor is isolated. When the set temperature is reached, the air is injected into the
132 reactor to achieve the required pressure of 15 MPa and the reaction begins ($t=0$). An
133 excess of oxygen of 70%, in comparison to the stoichiometry, is fixed at the beginning
134 of the reaction for each tested temperature, i.e. air ratio of 1.7 (Lefèvre et al. 2011a,
135 2011b). The agitation speed is set at 1000 rpm, which could permit to overcome mass
136 transfer limitations (Lefèvre et al., 2011a). The samples are collected at regular intervals
137 for glyphosate and TOC concentration analysis. The experiments at 473 and 523 K with
138 a reaction time of 15 and 30 min are repeated three times in order to obtain the standard
139 error.

140

141 2.3 Analytical methods

142 pH determined by pH meter (HACH Sension+ PH3). TOC concentration is
143 calculated from the difference between total carbon concentration and inorganic carbon
144 concentration measured by a TOC-L SHIMADZU analyser.

145 The possible organic intermediates of glyphosate degradation reported in the
146 literature are AMPA, glyoxylic acid, sarcosine and formaldehyde (Aquino Neto and de
147 Andrade, 2009; Balci et al., 2009; Echavia et al., 2009; Lan et al., 2013; Xing et al.,
148 2018). The detection of sarcosine is performed by a specific test kit (Biovision kit
149 Sarcosine, K636-100) with the maximum absorption wavelength (λ) of 570 nm. HCHO
150 is measured by UV-vis spectrophotometry by Spectroquant[®] test kit (1.14678.0001,
151 Merch Chemicals) at $\lambda=565$ nm.

152 The concentrations of glyphosate, AMPA and glyoxylic acid are determined by

153 LC/MS analysis. LC/MS analyses are performed using an Agilent 1290 Infinity system
154 coupled to an Agilent 6530 Q-TOF tandem mass spectrometer equipped with an Agilent
155 jet stream ion source. Instrument control, data analysis, and processing are performed
156 using Mass Hunter workstation software B4.00. The analysis method is adapted from
157 Yoshioka et al. (2011). Briefly, 1 μL of sample is injected and separation is performed
158 by using an Obelisc N column (150 mm x 2.1 mm internal diameter, 5 μm) distributed
159 by SIELC Technologies (Interchim, France). The mobile phase is composed of
160 acetonitrile/water (20/80, v/v) acidified with 0.1% formic at a flow rate of 0.2 $\text{mL}\cdot\text{min}^{-1}$.
161 The column is kept at 40 $^{\circ}\text{C}$ in the column oven. Mass calibration first performs pre-
162 acquisition using ESI-L low concentration tuning mix, provided by Agilent
163 technologies. Mass correction is performed by continuous calibration with hexakis (1H,
164 1H, 3H, tetrafluoropropoxy) phosphine and purine at m/z 922.0098 and m/z 121.0509
165 amu. After LC separation, the solution is introduced into the atmospheric pressure
166 ionization source and ionizes by electrospray in negative ion mode (ESI-) leading to
167 the formation of the $[\text{M} - \text{H}]^{-}$ ions of the analytes. Source parameters are set as follows:
168 fragmentor 140 V, capillary 3000 V, skimmer 65 V, and nitrogen is used as the drying
169 (350 $^{\circ}\text{C}$, 10 $\text{L}\cdot\text{min}^{-1}$), nebulizing (30 psi) and sheath (350 $^{\circ}\text{C}$, 8 $\text{L}\cdot\text{min}^{-1}$) gas. Scanning
170 is performed from m/z 50 to 1000 amu with 10,038 transients per spectrum.

171 For quantification of the three targeted analytes, Extracted Ion Current
172 chromatograms were used. Retention times, mass of deprotonated molecules and
173 Extracted Ion Current target molecular weight ranges shown between brackets are as
174 follows: glyoxylic acid (3.400 min, 72.9943 amu, [72.8-73.2 amu]), AMPA (3.695 min,

175 110.0032 amu, [109.8-110.2 amu]) and glyphosate (7.455 min, 168.0111 amu, [167.8-
176 168.2 amu]). The quantification of glyphosate, AMPA and glyoxylic acid
177 concentrations are based on linear regression ($R^2 > 0.999$) obtained by injecting standard
178 solutions containing the three analytes with concentrations ranging from 5-200 $\mu\text{g}\cdot\text{mL}^{-1}$.
179 ¹. Instrumental QC is performed by regular analyses of solvent blanks and random
180 injection of standards. Measured values are not deviating more than 15% from the
181 theoretical values. A rough estimation of the concentrations of other phosphorylated by-
182 products identified is performed by using the linear curve obtained for AMPA.

183 A screening of by-products is performed by working in Total Ion Current - MS
184 mode in order to determine molecular ions m/z. The chromatograms and their mass
185 spectra are inspected for transformation products known from the literature and for
186 unknown compounds. It should be underlined that none of the degradation products is
187 detected in the blank and standard. The elemental compositions are further calculated,
188 the maximum deviation was set to 10 ppm and C, H, N, O, P were selected as possible
189 present elements.

190 PO_4^{3-} , NH_4^+ , and NO_3^- are reported as possible inorganic degradation by-products
191 of glyphosate (Aquino Neto and de Andrade, 2009; Manassero et al., 2010; Lan et al.,
192 2013; Ndjeri et al., 2013). PO_4^{3-} is quantified by UV-vis spectroscopy through using
193 Spectroquant[®] test kit (1.00798.0001, Merck Chemicals) at $\lambda=690$ nm. NH_4^+ is detected
194 by UV-vis spectrophotometry through using Spectroquant[®] test kit (1.14752.0001,
195 Merck Chemicals) at $\lambda=690$ nm. NO_3^- is measured by UV-vis spectroscopy
196 (Spectroquant[®] test kit 1.09713.0001, Merck Chemicals) with $\lambda=340$ nm.

197 3 Results and discussion

198 3.1 Glyphosate degradation

199 In order to check the possible thermal degradation of glyphosate under the three
200 temperatures, the glyphosate concentrations are measured when the required
201 temperature is achieved and before oxygen injection. Different thermal degradations of
202 glyphosate under the three temperatures are found. The glyphosate concentration after
203 thermal degradation decreases from 1000 to 915.56, 754.00 and 459.00 mg L⁻¹, in
204 correspondence with TOC decreasing from 213 to 210.5, 178.1 and 159.3 mg L⁻¹, under
205 temperatures of 423, 473 and 523 K, respectively. Thus, the initial concentrations of
206 glyphosate and TOC for oxidation under the three temperatures are revised to the
207 concentration after thermal degradation. Then the glyphosate and TOC removal
208 (oxidation) is calculated by the following equation:

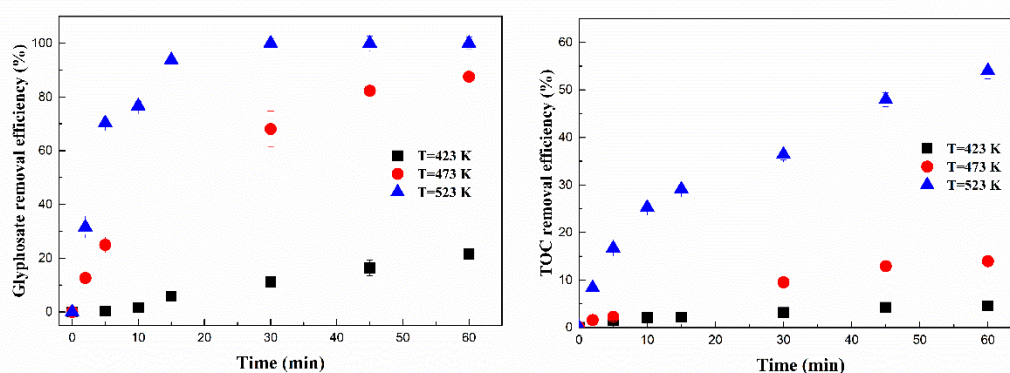
$$209 \quad \text{Removal (\%)} = \frac{(C_0 - C_t)}{C_0} \times 100\% \quad (1)$$

210 where C_0 is the initial concentration of glyphosate or TOC after revision (mg L⁻¹) and
211 C_t is the concentration at time t (mg L⁻¹).

212 The experimental results of glyphosate removal with time under three
213 temperatures are shown in Fig. 1. At 523 K, during the first 5 min of reaction, the
214 temperature in the cell increases up to 2 to 3°C due to exothermicity and then stabilizes
215 at 523 K thanks to the regulation system. The reaction temperature has a major effect
216 on the degradation of glyphosate. The glyphosate removal significantly increases with
217 an increase in temperature. At 523 K, complete glyphosate removal is obtained after 30
218 min. However, the removal of glyphosate is 87.6% and 21.4% after 60 min at 473 and

219 423 K, respectively. Furthermore, the results show that glyphosate is quickly degraded
 220 at 473 and 523 K, but slowly at 423 K, indicating that there seems to be a threshold
 221 between 423 and 473 K due to the significant gap in terms of degradation.

222 As some intermediate products appear during the oxidation of glyphosate to CO₂,
 223 it would be convenient for WAO design purposes to present its lumped parameter, i.e.,
 224 TOC. The effect of the temperature on the TOC removal is shown in Fig. 1. During the
 225 reaction time, the TOC decreases following the same pattern as for glyphosate removal.
 226 For instance, after 60 min, the TOC removal is 4.5%, 14% and 54% at 423, 473 and
 227 523 K, respectively. At the same reaction time, the TOC removal is smaller than
 228 glyphosate removal. This is attributed to the formation of low-molecular-weight and
 229 refractory intermediates, which remain in the solution and are not oxidized (Mishra et
 230 al., 1995; Vicente et al., 2002), especially at temperature below 473 K. Between 473
 231 and 523 K, there is a considerable performance gap for TOC abatement, indicating that
 232 the intermediates of glyphosate are more degradable at 523 K than that at 473 K.



233

234 Fig. 1 Effect of temperature on glyphosate and TOC removal efficiencies at 15 MPa

235 Regarding reaction intermediates, the formation of oxidation by-products of
 236 glyphosate in WAO process is further confirmed by the effluent pH. During glyphosate

237 oxidation by WAO process, the pH increases from 2.5 to 2.6, 3.0 and 4.1 after 60 min
238 at 423, 473 and 523 K, respectively. The increase of pH after oxidation is also found by
239 Xing et al. (2018). The highest pH value is obtained for the highest temperature,
240 indicating a faster elimination of glyphosate and its intermediates. This trend is opposite
241 to other literature dealing with other compounds, which found a pH decrease with the
242 increase in temperature caused by the formation of organic acids as reaction
243 intermediates (García-Molina et al., 2007; Suárez-Ojeda et al., 2007). In our case, this
244 is probably due to the generation of PO_4^{3-} during glyphosate oxidation as confirmed by
245 UV-vis spectrometry. For instance, the concentration of PO_4^{3-} ranged from 5.9 to 99.8
246 mg L^{-1} with the temperature increasing from 423 to 523 K after 30 min. PO_4^{3-} presents
247 alkaline properties in aqueous solution, causing the increase of pH.

248 3.2 Kinetic modelling

249 The global kinetic model tested, considering the concentration of organic
250 compounds and oxygen, has been validated by other authors for the treatment of organic
251 compounds and different wastewaters by WAO process (Lefèvre et al., 2011a; Li et al.,
252 1991; Rivas et al., 1998; Shende and Levec, 1999). The resulting mass balance in the
253 batch reactor is given through Equation 2.

$$254 \quad r = -\frac{dC}{dt} = kC^n C_{O_2}^m \quad (2)$$

255 where C is the concentration of organic compound; C_{O_2} is the concentration of oxygen
256 dissolved in the liquid phase; n and m are the partial orders; k is the rate constant,
257 which depends on Arrhenius equation (Equation 3).

$$258 \quad k = k_0 e^{-Ea/RT} \quad (3)$$

259 where k_0 is the pre-exponential factor; E_a is the activation energy for the reaction
260 (kJ mol^{-1}), R is the gas constant ($8.314 \text{ J mol}^{-1} \text{ K}^{-1}$) and T is the temperature (K).

261 In most cases for the oxidation of organic compounds by WAO process, a first
262 order with respect to the organic compound is found (Li et al., 1991; Shende and Levec,
263 1999). Thus, in this study, the order with respect to glyphosate is assumed to be first
264 order. Moreover, it is reported that if an excess oxygen is maintained at a constant partial
265 pressure in the reactor, the zero-order is respected for oxygen and the oxygen terms
266 may be assumed as a constant (Li et al., 1991; Kolaczowski et al., 1997; García-
267 Molina et al., 2007; Suárez-Ojeda et al., 2007). In this study, the air ratio is 1.7, ensuring
268 that oxygen is in excess. Thus, Equation 2 can be transferred to Equation 4.

$$269 \quad r = -\frac{dc}{dt} = kC \quad (4)$$

270 Equation 4 can be integrated to give Equation 5 to obtain the rate constant, k .

$$271 \quad \ln(C/C_0) = kt \quad (5)$$

272 Then, Equation 3 is transformed with logarithm to obtain the following expression:

$$273 \quad \ln k = \ln k_0 - E_a/RT \quad (6)$$

274 Thus, through linear regression, k_0 and E_a are obtained. In this study, C_0 and C
275 represent the initial concentration of glyphosate and glyphosate concentration at time t
276 (mM).

277

278

279

280

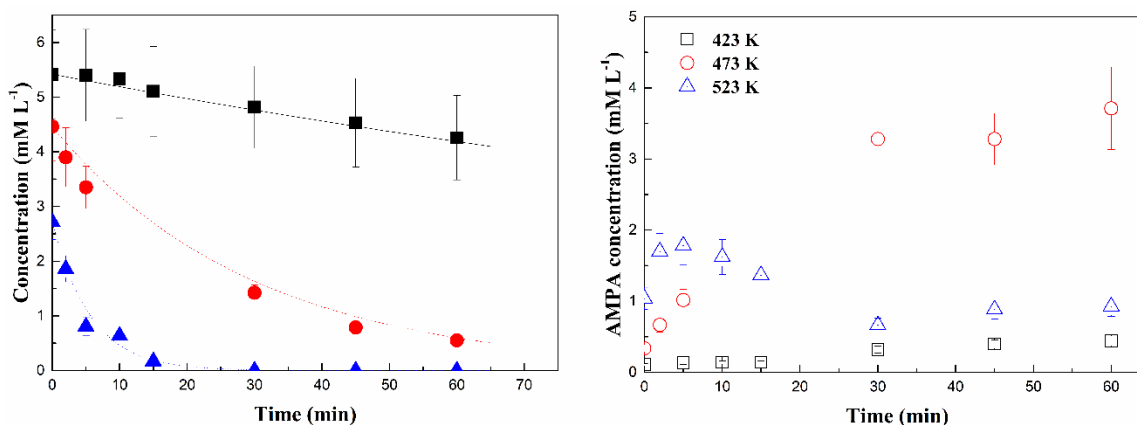
281 Table 1 Estimations of rate constant, pre-exponential factor and activation energy for
282 glyphosate oxidation

<i>T</i> (K)	<i>k</i> (min ⁻¹)	<i>R</i> ²	<i>k</i> ₀ (min ⁻¹)	<i>E</i> _a (kJ mol ⁻¹)
423	0.0042	0.991		
473	0.035	0.995	1212.3	68.4
523	0.17	0.954		

283

284 Table 1 shows that the first-order kinetic reaction fits well the glyphosate
285 degradation. The apparent reaction constants are presented in Table 1. It indicates that
286 glyphosate degradation rate increases significantly with an increase in temperature,
287 which is corroborated by the literature (Lei et al., 2007; Lin et al., 1996). Furthermore,
288 the apparent reaction constants are found to well agree with the Arrhenius equation (Fig.
289 S2) with *R*² of 0.99. The activation energy for glyphosate oxidation is estimated through
290 Arrhenius equation at 68.4 kJ mol⁻¹, which is in the upper range of those published for
291 WAO treatment of other organic compounds (33.1-77.8 kJ mol⁻¹) (Helling et al., 1981;
292 Joglekar et al., 1991; Lefèvre et al., 2011a; Pruden and Le, 1976; Suárez-Ojeda et al.,
293 2007). However, this value is well below those found in the literature for some small
294 organic molecules, such as acetic acid (167.7 kJ mol⁻¹), formic acid (121.3 kJ mol⁻¹), or
295 oxalic acid (129.4-133.8 kJ mol⁻¹) (Foussard Jean-Noël et al., 1989; Shende and
296 Mahajani, 1997, 1994). For most WAO process, organic compounds is inclined to
297 oxidize to these small molecules instead of CO₂ and H₂O (Lei et al., 2007). In this study,
298 the low activation energy indicates that glyphosate is more likely to be oxidized to
299 various intermediates.

300 A comparison of the glyphosate concentrations as a function of time obtain from
 301 the results of kinetic experiments with those calculated from the kinetic models is
 302 presented in Fig. 2. It can be seen that for the three temperatures studied, the model
 303 shows a good fit to the experimental points.



304

305 Fig. 2 Experimental and simulated concentration of glyphosate (left) and experimental
 306 generated AMPA concentration (right) during the experimental process: (1) ■: Experimental
 307 glyphosate concentration at 423 K; (2) ●: Experimental glyphosate concentration at 473 K; (3)
 308 ▲: Experimental glyphosate concentration at 523 K; (4) Solid line (—): Simulated glyphosate
 309 concentration at 423 K (5) Dash line (---): Simulated glyphosate concentration at 473 K; (6)
 310 Dot line (···): Simulated glyphosate concentration at 523 K; (7) □: AMPA concentration at 423
 311 K; (8) ○: AMPA concentration at 473 K; (9) △: AMPA concentration at 523 K.

312

313 3.3 Formation of by-products

314 To further understand the reaction mechanisms involved for glyphosate
 315 degradation by WAO process, by-product evaluation is required. Due to the complex
 316 variety of oxidation products, it is difficult to identify and quantify all the intermediates.
 317 However, some major stable oxidation by-products are measured to propose a possible
 318 degradation pathway of glyphosate via WAO. Some oxidation by-products of
 319 glyphosate in WAO process are confirmed by LC-MS or UV-vis spectrophotometry.
 320 Sarcosine is not detected in the samples by UV-vis spectrophotometer. AMPA, a most

321 frequently detected primary by-product of glyphosate in water, soil and oxidation
 322 treatments (Assalin et al., 2009; Echavia et al., 2009; Xing et al., 2018), is also detected
 323 in our study by using LC/MS analysis at the m/z ratio of 110.0032 amu. The
 324 concentrations of AMPA generated under three temperatures are presented in Fig. 2. It
 325 shows that at 423 K, low removal of glyphosate is obtained with little AMPA formed;
 326 at 473 K, high removal of glyphosate is achieved and almost all removed glyphosate is
 327 transformed into AMPA; complete glyphosate degradation is achieved and the AMPA
 328 generated at the beginning of the reaction is further degraded into other by-products
 329 over time at 523 K.

330 To further understand the relationship between glyphosate degradation and AMPA
 331 formation, glyphosate degradation, AMPA yield and relative yield of AMPA (described
 332 as the ratio of the molar quantity of AMPA generated, divided by the molar quantity of
 333 glyphosate removed) are calculated by equations 7-9.

$$334 \quad \text{Glyphosate degradation (\%)} = \frac{n_{\text{GLY}}^0 - n_{\text{GLY}}^t}{n_{\text{GLY}}^0} \times 100 \quad (7)$$

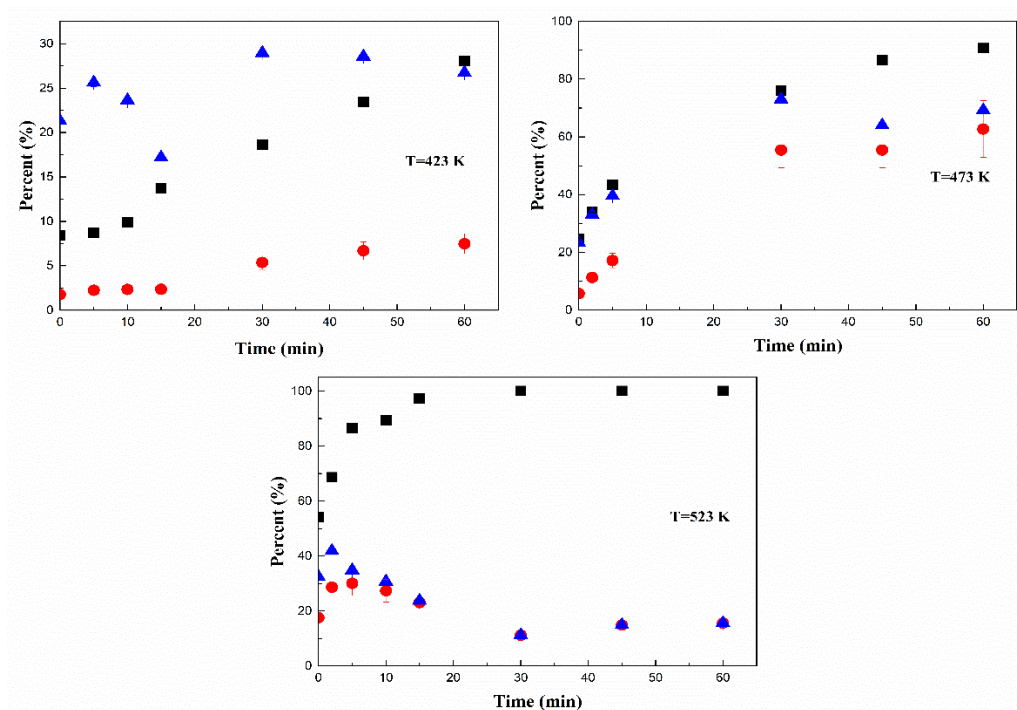
$$335 \quad \text{AMPA yield (\%)} = \frac{n_{\text{AMPA}}}{n_{\text{GLY}}^0} \times 100 \quad (8)$$

$$336 \quad \text{Relative yield (\%)} = \frac{n_{\text{AMPA}}}{n_{\text{GLY}}^0 - n_{\text{GLY}}^t} \times 100 \quad (9)$$

337 where n_{GLY}^0 is the initial glyphosate quantity (mol, with respect to the initial
 338 concentration of 1 g.L⁻¹); n_{GLY}^t is the glyphosate quantity at time t (mol); n_{AMPA} is
 339 the AMPA quantity at time t (mol).

340 The results of glyphosate degradation, AMPA yield and relative yield of AMPA
 341 under three temperatures are shown in Fig. 3. This figure shows that AMPA yield
 342 increases with respect to the increase of glyphosate degradation at 423 and 473 K, while

343 it first increases then decreases at 523 K. This indicates that AMPA is the primary
 344 product of glyphosate and can be further degraded at high temperature. Moreover, the
 345 relative yield of AMAP is close to 70% at 473 K, demonstrating that AMPA is the major
 346 transformation product of glyphosate at this temperature. The decrease of the relative
 347 yield to 15% at 523 K shows that by-products other than AMPA and containing the
 348 element P are mainly formed at this latter temperature.

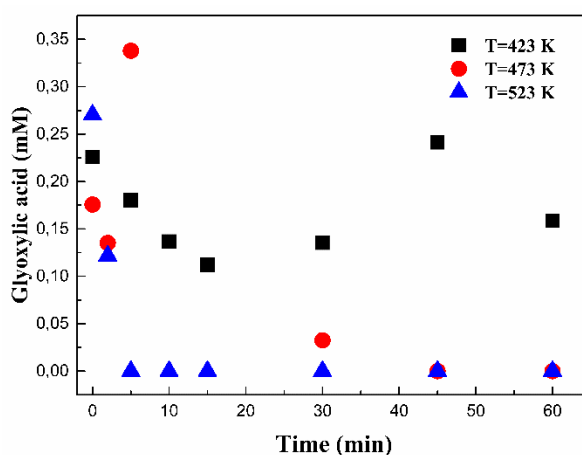


349
 350 Fig. 3 Glyphosate degradation (■), AMPA yield (●) and relative yield of AMPA (▲) during
 351 oxidation process at 423-523 K
 352

353 Furthermore, in order to further confirm the degradation of AMPA at 523 K, some
 354 kinetic experiments of AMPA degradation by WAO process are conducted using the
 355 same experimental procedure as for glyphosate (see section 2.2), with an initial AMPA
 356 concentration of 658 mg L⁻¹ corresponding to the same molar quantity as an initial
 357 glyphosate concentration of 1 g L⁻¹. The rate constant of AMPA degradation by WAO

358 process at 523 K is 0.01 mM min^{-1} with the half-life of 69.3 min (Fig. S3). After 60 min,
359 the removal efficiency of AMPA is 45.7%, which is lower than glyphosate removal for
360 the same conditions, indicating that AMPA is more resistant to degradation than
361 glyphosate, which is consistent with Xing et al. (2018).

362 The LC-MS analysis also reveal the presence of glyoxylic acid with m/z of
363 72.9943 amu. Fig. 4 shows the formation of glyoxylic acid during WAO degradation of
364 glyphosate. A low but almost constant concentration of glyoxylic acid is measured at
365 423 K, while at 473 and 523 K, its concentration first increases and then decreases until
366 it tends towards 0; this fall being particularly fast at 523 K. This suggests a quick further
367 oxidation of glyoxylic acid at higher temperatures. It was indeed reported that glyoxylic
368 acid can be further oxidized into formic acid (HCOOH) and finally mineralized into
369 CO_2 (Balci et al., 2009; Echavia et al., 2009).



370

371 Fig. 4 The formation of glyoxylic acid in WAO degradation of glyphosate.

372

373

374

375 Table 2 Concentration of by-products of glyphosate in the WAO process under three
376 temperatures after 30 min

T (K)	AMPA (mg L ⁻¹)	PO ₄ ³⁻ (mg L ⁻¹)	NH ₄ ⁺ (mg L ⁻¹)	NO ₃ ⁻ (mg L ⁻¹)	HCHO (mg L ⁻¹)
423	35.4	5.9	-	2.7	3.1
473	364.0	41.1	-	2.5	42.2
523	73.4	99.8	9.2	2.6	35.4

377 Table 2 shows the concentration of other by-products from glyphosate, such as
378 PO₄³⁻, NH₄⁺, NO₃⁻, and HCHO, in WAO conditions under three temperatures after 30
379 min. It indicates that the concentration of PO₄³⁻ increases with reaction temperature,
380 which is inconsistent with the destruction of glyphosate, implying that PO₄³⁻ is not
381 transformed directly from glyphosate, but rather from AMPA. Considering the element
382 N in AMPA, NH₄⁺ (Echavia et al., 2009; Ndjeri et al., 2013; Xing et al., 2018), which
383 is frequently reported as one of the final mineralization product of AMPA, is only
384 formed at 523 K. But the mass of N in the produced NH₄⁺ is not equal to the mass of N
385 in the AMPA degraded, indicating the presence of reaction intermediates between
386 AMPA and NH₄⁺. From recent literature (Annett et al., 2014; Fu et al., 2017),
387 methylamine (CH₃NH₂) has been reported as the intermediate during the degradation
388 of AMPA to NH₄⁺, which is also possible in our case, but this is not confirmed by
389 measuring it. The concentrations of NO₃⁻ under three temperatures are almost the same
390 and equal to the initial glyphosate solution, indicating that NO₃⁻ is not the final
391 mineralization product of glyphosate in our experiments. It is probably due to the short
392 reaction time, which is not enough to further oxidize the generated NH₄⁺ into NO₃⁻.
393 Furthermore, the concentration of HCHO increased significantly with the increase in

394 reaction temperature from 423 K to 473 K. As for each mole of glyphosate decomposed,
395 the yield of AMPA and HCHO is not equivalent, it is supposed that glyphosate was not
396 directly degraded into HCHO. The concentration of HCHO is approximately the same
397 as the concentration of PO_4^{3-} . This equality may indicate that HCHO and PO_4^{3-} are
398 directly formed through the degradation of AMPA, which is consistent with the results
399 obtained by Xing et al. (2018). When the temperature further increases to 523 K, the
400 concentration of HCHO decreases, indicating that HCHO can be further oxidized to
401 other by-products at the highest temperature. HCOOH intermediate and final
402 mineralization into CO_2 has been previously reported (Manassero et al., 2010; Xing et
403 al., 2018; Yang et al., 2018).

404 3.4 Proposed degradation pathway

405 A degradation pathway of glyphosate in WAO conditions (Fig. 5) is proposed
406 considering the evaluation of major intermediates and final products based on
407 experimental data. Previous studies have reported that glyphosate oxidation often
408 follows two mechanisms, which are related to the cleavage of C-N and C-P bonds to
409 generate AMPA and sarcosine, respectively (Barrett and McBride, 2005; Manassero et
410 al., 2010; Paudel et al., 2015; Yang et al., 2018). In this work, the existence of AMPA
411 and glyoxylic acid and the absence of sarcosine indicate that the glyphosate degradation
412 by WAO conditions followed the mechanism of C-N bond cleavage. First, the C-N bond
413 of glyphosate promoted by OH attack is broken and yield to AMPA, and glyoxylic acid.
414 Glyoxylic acid is further oxidized into HCOOH. Then C-P bond cleavage of AMPA
415 generated PO_4^{3-} , HCHO, and methylamine (CH_3NH_2). Methylamine is further oxidized

416 into NH_4^+ and HCHO. WAO conditions generally involve the oxidation of NH_4^+ into
 417 NO_3^- and the oxidation of HCHO into HCOOH, and further into CO_2 and H_2O . As these
 418 final products were not detected in this work, these transformations are reported with
 419 dotted arrow on the pathway scheme of Fig. 5.

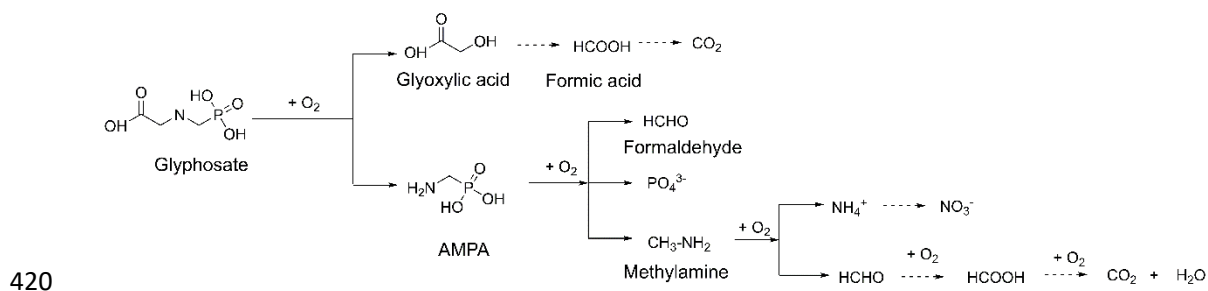


Fig. 5 A proposed degradation pathway of glyphosate for WAO conditions

422 4 Conclusions

423 WAO process is an effective technique to treat effluents containing glyphosate
 424 since complete glyphosate removal and 54% of TOC reduction was obtained at 523 K
 425 and 15 MPa after 60 min. The glyphosate oxidation obeys first-order kinetics with
 426 respect to glyphosate concentration. The degradation rate is faster when increasing the
 427 reaction temperature. The activation energy is 68.4 kJ mol^{-1} . Some possible by-products
 428 of glyphosate in WAO process are identified and a degradation pathway is proposed.
 429 This study proposes a kinetic scheme which can be easily implemented in a WAO
 430 process simulation in order to obtain a first evaluation of the process functioning.
 431 Further work to consider the kinetic scheme with by-products of glyphosate should be
 432 studied to have more accurate information on WAO process.

433 **Acknowledgments**

434 The authors would like to express their thanks to the Chinese Scholarship Council
435 (File No. 201604490033) for financing this work. They also thank very much Jean-Paul
436 Nisteron and Stéphanie Lebarillier for technical support on the experimental work.

437 **References**

- 438 Annett, R., Habibi, H.R., Hontela, A., 2014. Impact of glyphosate and glyphosate-based
439 herbicides on the freshwater environment. *J. Appl. Toxicol.* JAT 34, 458–479.
440 <https://doi.org/10.1002/jat.2997>
- 441 Aquino Neto, S., de Andrade, A.R., 2009. Electrooxidation of glyphosate herbicide at
442 different DSA® compositions: pH, concentration and supporting electrolyte
443 effect. *Electrochimica Acta* 54, 2039–2045.
444 <https://doi.org/10.1016/j.electacta.2008.07.019>
- 445 Assalin, M.R., Moraes, S.G.D., Queiroz, S.C.N., Ferracini, V.L., Duran, N., 2009.
446 Studies on degradation of glyphosate by several oxidative chemical processes:
447 Ozonation, photolysis and heterogeneous photocatalysis. *J. Environ. Sci. Health*
448 *Part B* 45, 89–94. <https://doi.org/10.1080/03601230903404598>
- 449 Balci, B., Oturan, M.A., Oturan, N., Sirés, I., 2009. Decontamination of aqueous
450 glyphosate, (aminomethyl)phosphonic acid, and glufosinate solutions by
451 electro-Fenton-like process with Mn_2^+ as the catalyst. *J. Agric. Food Chem.* 57,
452 4888–4894. <https://doi.org/10.1021/jf900876x>
- 453 Barrett, K.A., McBride, M.B., 2005. Oxidative degradation of glyphosate and
454 aminomethylphosphonate by Manganese oxide. *Environ. Sci. Technol.* 39,
455 9223–9228. <https://doi.org/10.1021/es051342d>
- 456 Baylis, A.D., 2000. Why glyphosate is a global herbicide: strengths, weaknesses and
457 prospects. *Pest Manag. Sci.* 56, 299–308. [https://doi.org/10.1002/\(SICI\)1526-4998\(200004\)56:4<299::AID-PS144>3.0.CO;2-K](https://doi.org/10.1002/(SICI)1526-4998(200004)56:4<299::AID-PS144>3.0.CO;2-K)
- 459 Chen, S., Liu, Y., 2007. Study on the photocatalytic degradation of glyphosate by TiO₂
460 photocatalyst. *Chemosphere* 67, 1010–1017.
461 <https://doi.org/10.1016/j.chemosphere.2006.10.054>
- 462 Chen, Y., Wu, F., Lin, Y., Deng, N., Bazhin, N., Glebov, E., 2007. Photodegradation of
463 glyphosate in the ferrioxalate system. *J. Hazard. Mater.* 148, 360–365.
464 <https://doi.org/10.1016/j.jhazmat.2007.02.044>
- 465 Debellefontaine, H., Foussard, J.N., 2000. Wet air oxidation for the treatment of
466 industrial wastes. Chemical aspects, reactor design and industrial applications
467 in Europe. *Waste Manag.* 20, 15–25. [https://doi.org/10.1016/S0956-053X\(99\)00306-2](https://doi.org/10.1016/S0956-053X(99)00306-2)
- 469 Demirel, M., Kayan, B., 2012. Application of response surface methodology and central
470 composite design for the optimization of textile dye degradation by wet air

471 oxidation. *Int. J. Ind. Chem.* 3, 24. <https://doi.org/10.1186/2228-5547-3-24>

472 Devlin, H.R., Harris, I.J., 1984. Mechanism of the oxidation of aqueous phenol with
473 dissolved oxygen. *Ind. Eng. Chem. Fundam.* 23, 387–392.
474 <https://doi.org/10.1021/i100016a002>

475 Echavia, G.R.M., Matzusawa, F., Negishi, N., 2009. Photocatalytic degradation of
476 organophosphate and phosphonoglycine pesticides using TiO₂ immobilized on
477 silica gel. *Chemosphere* 76, 595–600.
478 <https://doi.org/10.1016/j.chemosphere.2009.04.055>

479 Fan, J., Yang, G., Zhao, H., Shi, G., Geng, Y., Hou, T., Tao, K., 2012. Isolation,
480 identification and characterization of a glyphosate-degrading bacterium,
481 *Bacillus cereus* CB4, from soil. *J. Gen. Appl. Microbiol.* 58, 263–271.

482 Feng, D., Ferrasse, J.-H., Soric, A., Boutin, O., 2019. Bubble characterization and gas–
483 liquid interfacial area in two phase gas–liquid system in bubble column at low
484 Reynolds number and high temperature and pressure. *Chem. Eng. Res. Des.* 144,
485 95–106. <https://doi.org/10.1016/j.cherd.2019.02.001>

486 Firdous, S., Iqbal, S., Anwar, S., 2017. Optimization and modeling of glyphosate
487 biodegradation by a novel *comamonas odontotermitis* P2 Through Response
488 Surface Methodology. *Pedosphere.* [https://doi.org/10.1016/S1002-](https://doi.org/10.1016/S1002-0160(17)60381-3)
489 [0160\(17\)60381-3](https://doi.org/10.1016/S1002-0160(17)60381-3)

490 Foussard Jean-Noël, Debellefontaine Hubert, Besombes-Vailhé Jean, 1989. Efficient
491 elimination of organic liquid wastes: wet air oxidation. *J. Environ. Eng.* 115,
492 367–385. [https://doi.org/10.1061/\(ASCE\)0733-9372\(1989\)115:2\(367\)](https://doi.org/10.1061/(ASCE)0733-9372(1989)115:2(367))

493 Fu, G., Chen, Y., Li, R., Yuan, X., Liu, C., Li, B., Wan, Y., 2017. Pathway and rate-
494 limiting step of glyphosate degradation by *Aspergillus oryzae* A-F02. *Prep.*
495 *Biochem. Biotechnol.* 47, 782–788.
496 <https://doi.org/10.1080/10826068.2017.1342260>

497 García-Molina, V., Kallas, J., Esplugas, S., 2007. Wet oxidation of 4-chlorophenol:
498 Kinetic study. *Chem. Eng. J.* 126, 59–65.
499 <https://doi.org/10.1016/j.cej.2006.05.022>

500 Gill, J.P.K., Sethi, N., Mohan, A., 2017. Analysis of the glyphosate herbicide in water,
501 soil and food using derivatising agents. *Environ. Chem. Lett.* 15, 85–100.
502 <https://doi.org/10.1007/s10311-016-0585-z>

503 Guilherme, S., Gaivão, I., Santos, M.A., Pacheco, M., 2010. European eel (*Anguilla*
504 *anguilla*) genotoxic and pro-oxidant responses following short-term exposure to
505 Roundup--a glyphosate-based herbicide. *Mutagenesis* 25, 523–530.
506 <https://doi.org/10.1093/mutage/geq038>

507 Hadi, F., Mousavi, A., Noghabi, K.A., Tabar, H.G., Salmanian, A.H., 2013. New
508 bacterial strain of the genus *Ochrobactrum* with glyphosate-degrading activity.
509 *J. Environ. Sci. Health Part B* 48, 208–213.
510 <https://doi.org/10.1080/03601234.2013.730319>

511 Heitkamp, M.A., Adams, W.J., Hallas, L.E., 1992. Glyphosate degradation by
512 immobilized bacteria: laboratory studies showing feasibility for glyphosate
513 removal from waste water. *Can. J. Microbiol.* 38, 921–928.
514 <https://doi.org/10.1139/m92-149>

515 Helling, R.K., Strobel, M.K., Torres, R.J., 1981. Kinetics of wet oxidation of biological
516 sludges from coal-conversion wastewater treatment (No. ORNL/MIT-332). Oak
517 Ridge National Lab., TN (USA); Massachusetts Inst. of Tech., Oak Ridge, TN
518 (USA). School of Chemical Engineering Practice.

519 Herath, I., Kumarathilaka, P., Al-Wabel, M.I., Abduljabbar, A., Ahmad, M., Usman,
520 A.R.A., Vithanage, M., 2016. Mechanistic modeling of glyphosate interaction
521 with rice husk derived engineered biochar. *Microporous Mesoporous Mater.*
522 225, 280–288. <https://doi.org/10.1016/j.micromeso.2016.01.017>

523 Hu, X., Lei, L., Chen, G., Yue, P.L., 2001. On the degradability of printing and dyeing
524 wastewater by wet air oxidation. *Water Res.* 35, 2078–2080.
525 [https://doi.org/10.1016/S0043-1354\(00\)00481-4](https://doi.org/10.1016/S0043-1354(00)00481-4)

526 Joglekar, H.S., Samant, S.D., Joshi, J.B., 1991. Kinetics of wet air oxidation of phenol
527 and substituted phenols. *Water Res.* 25, 135–145. [https://doi.org/10.1016/0043-1354\(91\)90022-I](https://doi.org/10.1016/0043-1354(91)90022-I)

529 Kim, K.-H., Ihm, S.-K., 2011. Heterogeneous catalytic wet air oxidation of refractory
530 organic pollutants in industrial wastewaters: A review. *J. Hazard. Mater.* 186,
531 16–34. <https://doi.org/10.1016/j.jhazmat.2010.11.011>

532 Kolaczowski, S.T., Beltran, F.J., McLurgh, D.B., Rivas, F.J., 1997. Wet air oxidation
533 of phenol: factors that may influence global kinetics. *Process Saf. Environ. Prot.*
534 75, 257–265. <https://doi.org/10.1205/095758297529138>

535 Lan, H., Jiao, Z., Zhao, X., He, W., Wang, A., Liu, H., Liu, R., Qu, J., 2013. Removal
536 of glyphosate from water by electrochemically assisted MnO₂ oxidation
537 process. *Sep. Purif. Technol.* 117, 30–34.
538 <https://doi.org/10.1016/j.seppur.2013.04.012>

539 Lefèvre, S., Boutin, O., Ferrasse, J.-H., Malleret, L., Faucherand, R., Viand, A., 2011a.
540 Thermodynamic and kinetic study of phenol degradation by a non-catalytic wet
541 air oxidation process. *Chemosphere* 84, 1208–1215.
542 <https://doi.org/10.1016/j.chemosphere.2011.05.049>

543 Lefèvre, S., Ferrasse, J.-H., Boutin, O., Sergent, M., Faucherand, R., Viand, A., 2011b.
544 Process optimisation using the combination of simulation and experimental
545 design approach: Application to wet air oxidation. *Chem. Eng. Res. Des.* 89,
546 1045–1055. <https://doi.org/10.1016/j.cherd.2010.12.009>

547 Lefevre, S., Ferrasse, J.-H., Faucherand, R., Viand, A., Boutin, O., 2012. Energetic
548 optimization of wet air oxidation process using experimental design coupled
549 with process simulation. *Energy, 23rd International Conference on Efficiency,
550 Cost, Optimization, Simulation and Environmental Impact of Energy Systems,
551 ECOS 2010* 41, 175–183. <https://doi.org/10.1016/j.energy.2011.09.043>

552 Lei, L., Dai, Q., Zhou, M., Zhang, X., 2007. Decolorization of cationic red X-GRL by
553 wet air oxidation: Performance optimization and degradation mechanism.
554 *Chemosphere* 68, 1135–1142.
555 <https://doi.org/10.1016/j.chemosphere.2007.01.075>

556 Leonard, C., Ferrasse, J.-H., Boutin, O., Lefevre, S., Viand, A., 2015. Bubble column
557 reactors for high pressures and high temperatures operation. *Chem. Eng. Res.
558 Des.* 100, 391–421. <https://doi.org/10.1016/j.cherd.2015.05.013>

559 Leonard, C., Ferrasse, J.-H., Lefevre, S., Viand, A., Boutin, O., 2019. Gas hold up in
560 bubble column at high pressure and high temperature. *Chem. Eng. Sci.* 200,
561 186–202. <https://doi.org/10.1016/j.ces.2019.01.055>

562 Levec, J., Pintar, A., 2007. Catalytic wet-air oxidation processes: A review. *Catal. Today*,
563 *Advanced Catalytic Oxidation Processes* 124, 172–184.
564 <https://doi.org/10.1016/j.cattod.2007.03.035>

565 Li, L., Chen, P., Gloyna, E.F., 1991. Generalized kinetic model for wet oxidation of
566 organic compounds. *AIChE J.* 37, 1687–1697.
567 <https://doi.org/10.1002/aic.690371112>

568 Lin, S.H., Ho, S.J., Wu, C.L., 1996. Kinetic and performance characteristics of wet air
569 oxidation of high-concentration wastewater. *Ind. Eng. Chem. Res.* 35, 307–314.
570 <https://doi.org/10.1021/ie950251u>

571 Liu, Z., Zhu, M., Yu, P., Xu, Y., Zhao, X., 2013. Pretreatment of membrane separation
572 of glyphosate mother liquor using a precipitation method. *Desalination* 313,
573 140–144. <https://doi.org/10.1016/j.desal.2012.12.011>

574 Luck, F., 1999. Wet air oxidation: past, present and future. *Catal. Today* 53, 81–91.
575 [https://doi.org/10.1016/S0920-5861\(99\)00112-1](https://doi.org/10.1016/S0920-5861(99)00112-1)

576 Manassero, A., Passalia, C., Negro, A.C., Cassano, A.E., Zalazar, C.S., 2010.
577 Glyphosate degradation in water employing the H₂O₂/UVC process. *Water Res.*
578 44, 3875–3882. <https://doi.org/10.1016/j.watres.2010.05.004>

579 Mantzavinos, D., Livingston, A.G., Hellenbrand, R., Metcalfe, I.S., 1996. Wet air
580 oxidation of polyethylene glycols; mechanisms, intermediates and implications
581 for integrated chemical-biological wastewater treatment. *Chem. Eng. Sci.* 51,
582 4219–4235. [https://doi.org/10.1016/0009-2509\(96\)00272-2](https://doi.org/10.1016/0009-2509(96)00272-2)

583 Mishra, V.S., Mahajani, V.V., Joshi, J.B., 1995. Wet air oxidation. *Ind. Eng. Chem. Res.*
584 34, 2–48. <https://doi.org/10.1021/ie00040a001>

585 Ndjeri, M., Pensel, A., Peulon, S., Haldys, V., Desmazières, B., Chaussé, A., 2013.
586 Degradation of glyphosate and AMPA (amino methylphosphonic acid) solutions
587 by thin films of birnessite electrodeposited: A new design of material for
588 remediation processes? *Colloids Surf. Physicochem. Eng. Asp.* 435, 154–169.
589 <https://doi.org/10.1016/j.colsurfa.2013.01.022>

590 Paudel, P., Negusse, A., Jaisi, D.P., 2015. Birnessite-catalyzed degradation of
591 glyphosate: A mechanistic study aided by kinetics batch studies and NMR
592 spectroscopy. *Soil Sci. Soc. Am. J.* 79, 815–825.
593 <https://doi.org/10.2136/sssaj2014.10.0394>

594 Pruden, B.B., Le, H., 1976. Wet air oxidation of soluble components in waste water.
595 *Can. J. Chem. Eng.* 54, 319–325. <https://doi.org/10.1002/cjce.5450540413>

596 Rivas, F.J., Kolaczowski, S.T., Beltran, F.J., McLurgh, D.B., 1998. Development of a
597 model for the wet air oxidation of phenol based on a free radical mechanism -
598 ScienceDirect. *Chem. Eng. Sci.* 53, 2575–2586.

599 Sandy, E.H., Blake, R.E., Chang, S.J., Jun, Y., Yu, C., 2013. Oxygen isotope signature
600 of UV degradation of glyphosate and phosphonoacetate: Tracing sources and
601 cycling of phosphonates. *J. Hazard. Mater.* 260, 947–954.
602 <https://doi.org/10.1016/j.jhazmat.2013.06.057>

603 Shende, R.V., Levec, J., 1999. Kinetics of wet oxidation of propionic and 3-
604 hydroxypropionic acids. *Ind. Eng. Chem. Res.* 38, 2557–2563.
605 <https://doi.org/10.1021/ie9900061>

606 Shende, R.V., Mahajani, V.V., 1997. Kinetics of wet oxidation of formic acid and acetic
607 acid. *Ind. Eng. Chem. Res.* 36, 4809–4814. <https://doi.org/10.1021/ie970048u>

608 Shende, R.V., Mahajani, V.V., 1994. Kinetics of wet air oxidation of glyoxalic acid and
609 oxalic acid. *Ind. Eng. Chem. Res.* 33, 3125–3130.
610 <https://doi.org/10.1021/ie00036a030>

611 Suárez-Ojeda, M.E., Kim, J., Carrera, J., Metcalfe, I.S., Font, J., 2007. Catalytic and
612 non-catalytic wet air oxidation of sodium dodecylbenzene sulfonate: Kinetics
613 and biodegradability enhancement. *J. Hazard. Mater.*, " Selected papers of the
614 proceedings of the 5th European Meeting on Chemical Industry and
615 Environment, EMChIE 2006 " held in Vienna, Austria, 3-5 May 2006 144, 655–
616 662. <https://doi.org/10.1016/j.jhazmat.2007.01.091>

617 Vicente, J., Rosal, R., Díaz, M., 2002. Noncatalytic oxidation of phenol in aqueous
618 solutions. *Ind. Eng. Chem. Res.* 41, 46–51. <https://doi.org/10.1021/ie010130w>

619 Wang, M., Zhang, G., Qiu, G., Cai, D., Wu, Z., 2016. Degradation of herbicide
620 (glyphosate) using sunlight-sensitive MnO₂/C catalyst immediately fabricated
621 by high energy electron beam. *Chem. Eng. J.* 306, 693–703.
622 <https://doi.org/10.1016/j.cej.2016.07.063>

623 Watanabe, M., Inomata, H., Smith, R.L., Arai, K., 2001. Catalytic decarboxylation of
624 acetic acid with zirconia catalyst in supercritical water. *Appl. Catal. Gen.* 219,
625 149–156. [https://doi.org/10.1016/S0926-860X\(01\)00677-9](https://doi.org/10.1016/S0926-860X(01)00677-9)

626 Xie, M., Liu, Z., Xu, Y., 2010. Removal of glyphosate in neutralization liquor from the
627 glycine-dimethylphosphit process by nanofiltration. *J. Hazard. Mater.* 181, 975–
628 980. <https://doi.org/10.1016/j.jhazmat.2010.05.109>

629 Xing, B., Chen, H., Zhang, X., 2018. Efficient degradation of organic phosphorus in
630 glyphosate wastewater by catalytic wet oxidation using modified activated
631 carbon as a catalyst. *Environ. Technol.* 39, 749–758.
632 <https://doi.org/10.1080/09593330.2017.1310935>

633 Xing, B., Chen, H., Zhang, X., 2017. Removal of organic phosphorus and formaldehyde
634 in glyphosate wastewater by CWO and the lime-catalyzed formose reaction.
635 *Water Sci. Technol.* 75, 1390–1398. <https://doi.org/10.2166/wst.2017.006>

636 Yang, Y., Deng, Q., Yan, W., Jing, C., Zhang, Y., 2018. Comparative study of glyphosate
637 removal on goethite and magnetite: Adsorption and photo-degradation. *Chem.*
638 *Eng. J.* 352, 581–589. <https://doi.org/10.1016/j.cej.2018.07.058>

639 Yoshioka, N., Asano, M., Kuse, A., Mitsuhashi, T., Nagasaki, Y., Ueno, Y., 2011. Rapid
640 determination of glyphosate, glufosinate, bialaphos, and their major metabolites
641 in serum by liquid chromatography–tandem mass spectrometry using
642 hydrophilic interaction chromatography. *J. Chromatogr. A* 1218, 3675–3680.
643 <https://doi.org/10.1016/j.chroma.2011.04.021>

644